American Mineralogist, Volume 71, pages 977–984, 1986

High-pressure crystal chemistry of beryl ($Be_3Al_2Si_6O_{18}$) and euclase ($BeAlSiO_4OH$)

ROBERT M. HAZEN, ANDREW Y. AU, LARRY W. FINGER
Geophysical Laboratory, Carnegie Institution of Washington, 2801 Upton Street, N.W., Washington, D.C. 20008

ABSTRACT

Compressibilities and high-pressure crystal structures of beryl and euclase have been determined by X-ray methods at several pressures. Beryl (hexagonal, space group *P6/mcc*) has nearly isotropic compressibility; linear compressibilities perpendicular and parallel to the **c** axis are $\beta_\perp = 1.72 \pm 0.04 \times 10^{-4}$ kbar^{-1} and $\beta_\parallel = 2.10 \pm 0.09 \times 10^{-4}$ kbar^{-1}. The corresponding bulk modulus is 1.70 ± 0.05 Mbar if the pressure derivative of the bulk modulus K' is assumed to be 4. Euclase (monoclinic, space group $P2_1/a$) has anisotropic compression, with maximum compressibility of $2.44 \pm 0.05 \times 10^{-4}$ kbar^{-1} parallel to the unique monoclinic **b** axis, and minimum compressibility of $1.50 \pm 0.03 \times 10^{-4}$ kbar^{-1} approximately parallel to [101]. The intermediate axis of compression has a magnitude of $1.96 \pm 0.05 \times 10^{-4}$ kbar^{-1} in the **a**-**c** plane. The bulk modulus of euclase is 1.59 ± 0.03 Mbar if K' is assumed to be 4.

The bulk moduli of Be, Al, and Si cation coordination polyhedra in beryl are all consistent with 1.7 Mbar, which is the crystal bulk modulus. Beryl compression occurs primarily by shortening of cation–anion bond distances. In euclase, the 2.3-Mbar polyhedral bulk moduli are significantly greater than the observed 1.6-Mbar crystal modulus. Compression in euclase, particularly along the **b** crystallographic axis, results from a combination of polyhedral compression and changes in interpolyhedral angles.

INTRODUCTION

Among the more fundamental goals of mineralogy and petrology is the prediction of physical properties and phase equilibria from a knowledge of structure and bonding. The study of minerals must proceed on a broad front of experiment and theory if microscopic structural characteristics are to be related to macroscopic mineral behavior. One promising approach is the characterization and rationalization of properties—structural, thermochemical, elastic, and vibrational—for a group of closely related minerals. The system BeO-Al_2O_3-SiO_2-H_2O provides an ideal suite of large, well-formed, stoichiometric, and ordered crystalline phases in a variety of structure types. All atoms are of low atomic number and are thus amenable to the procedures of computational quantum chemistry. Only three types of cation coordination polyhedra—Be and Si tetrahedra and Al octahedra—provide the structural building blocks for most of the phases, thus facilitating tests of the "polyhedral approach" for modeling mineral properties (Hazen, 1985). Recent studies, completed as part of this integrated effort, include vibrational spectroscopy (Hoering and Hofmeister, 1985), elastic moduli (Au and Hazen, 1985; Yeganeh-Haeri and Weidner, 1986), thermochemistry (Barton, 1986), and comparative crystal chemistry (Hazen and Au, 1986). Also in progress are modeling of Be polyhedral clusters by ab initio molecular orbital procedures and lattice dynamic calculations for the oxides of Be, Al, and Si by modified electron-gas methods.

The crystal structure of beryl [$Be_3Al_2Si_6O_{18}$: hexagonal *P6/mcc*, $Z = 2$] has been reported by Gibbs et al. (1968) and Morosin (1972). It is characterized by six-member rings of Si tetrahedra, cross-linked by Be tetrahedra and Al octahedra (Fig. 1a). The tetrahedral rings lie in the (0001) plane and are superimposed to form channels along the **c** axis. Though often classified as a ring-silicate, beryl can also be described (Zoltai, 1960) as a three-dimensional framework of Be and Si tetrahedra (Fig. 1b).

The structure of euclase [$BeAlSiO_4(OH)$: monoclinic $P2_1/a$, $Z = 4$] was described by Mrose and Appleman (1962). Euclase has *a*-axis chains of three-member rings formed by interconnected Be and Si tetrahedra (Fig. 2a), cross-linked by Al octahedra (Fig. 2b). Although technically an orthosilicate with isolated Si tetrahedra, euclase can be interpreted equally well in terms of chains of Be and Si tetrahedra.

The principal objectives of this high-pressure research on beryl and euclase are (1) to determine pressure-volume equation-of-state parameters and compression anisotropies by measuring the pressure variation of unit-cell dimensions, (2) to calculate polyhedral bulk moduli from high-pressure structure data in order to test the effects of structure on these moduli, (3) to identify geometrical changes in the beryl and euclase structures that result in

0003–004X/86/0708–0977$02.00

Table 1. Unit-cell parameters of beryl and euclase at several pressures

BERYL

P(kbar)	2θ range+	a(Å)	c(Å)	V(Å^3)	c/a	V/V_o
0.001	45-55	9.214(1)*	9.194(1)	676.0(1)	0.9978	1.0016
0.001	25	9.208(3)	9.188(3)	674.7(3)	0.9978	1.0000
15	25	9.183(3)	9.159(3)	669.1(3)	0.9974	0.9918
18	25	9.179(2)	9.157(3)	668.2(3)	0.9976	0.9904
30	25	9.163(10)	9.131(5)	663.5(11)	0.9965	0.9835
33	25	9.155(3)	9.118(2)	661.6(3)	0.9960	0.9806
36	25	9.153(3)	9.119(1)	661.6(3)	0.9960	0.9806
40	25	9.138(10)	1.113(1)	659.2(5)	0.9973	0.9771
43	25	9.135(6)	9.103(2)	657.9(7)	0.9964	0.9752
47	25	9.134(4)	9.096(2)	657.0(3)	0.9958	0.9738
57	14	9.127(3)	9.064(15)	652.4(15)	0.9931	0.9670

EUCLASE

P(kbar)	a(Å)	b(Å)	c(Å)	β(°)	V(Å^3)	V/V_o
0.001	4.7800(3)	14.322(1)	4.6335(2)	100.310(5)	312.30(3)	1.0000
21	4.759(1)	14.255(6)	4.612(1)	100.24(1)	307.89(10)	0.9859
22	4.761(1)	14.254(4)	4.610(1)	100.27(1)	307.85(15)	0.9859
42	4.746(1)	14.189(11)	4.599(1)	100.18(2)	304.82(26)	0.9760
49	4.739(1)	14.158(3)	4.589(1)	100.15(1)	303.14(11)	0.9707
62	4.730(1)	14.136(9)	4.580(1)	100.16(2)	301.40(22)	0.9651

* Parenthesized figures represent esd's.
\+ Measured unit-cell parameters may depend systematically on the range of 2θ used in their determination (Swanson et al., 1985). Only 25° data were used in equation-of-state determinations.

Table 2. Beryl refinement conditions and refined atomic parameters

		1 bar	19 kbar	36 kbar	57 kbar
Number of Obs (I>2σ)		299	100	107	94
R(%)+		3.1	3.5	3.8	4.1
Weighted R(%)+		2.6	2.8	3.0	3.2
Extinction, r* (x10^5)		6.7(7)*	1.4(7)	5(1)	1.4(8)
Atom	Parameter				
Be	x	0.5	0.5	0.5	0.5
	y	0	0	0	0
	z	0.25	0.25	0.25	0.25
	B	0.57(7)	0.3(2)	0.4(3)	0.8(4)
Al	x	1/3	1/3	1/3	1/3
	y	2/3	2/3	2/3	2/3
	z	0.25	0.25	0.25	0.25
	B	0.51(3)	0.9(1)	1.1(1)	1.0(1)
Si	x	0.3876(1)	0.3882(3)	0.3883(3)	0.3893(4)
	y	0.1159(1)	0.1155(3)	0.1161(3)	0.1166(4)
	z	0	0	0	0
	B	0.44(3)	0.68(8)	0.87(8)	0.95(10)
O1	x	0.3103(3)	0.3122(6)	0.3111(6)	0.3107(8)
	y	0.2369(3)	0.2376(7)	0.2371(6)	0.2366(8)
	z	0	0	0	0
	B	0.82(5)	0.58(13)	1.06(14)	0.30(17)
O2	x	0.4985(2)	0.4987(4)	0.4984(5)	0.4992(6)
	y	0.1456(2)	0.1459(4)	0.1450(4)	0.1452(5)
	z	0.1453(1)	0.1449(5)	0.1447(5)	0.1470(6)
	B	0.68(3)	0.78(10)	0.98(10)	0.72(12)

* Parenthesized figures represent esd's
\+ $R = \Sigma[||F_o|-|F_c||]/\Sigma F_o$
Weighted $R = [\Sigma w(|F_o|-|F_c|)^2/\Sigma wF_o^2]^{1/2}$

compression, and (4) to relate structural changes in beryl at high pressure to the elastic moduli determined by Yoon and Newnham (1973).

Experimental methods

Specimen description

Crystals of synthetic beryl (variety emerald) were provided by Richard M. Mandle (Vacuum Ventures, Inc.). This material conforms to the ideal beryl composition, with the exception of 0.37 wt% Cr, corresponding to 1.3% occupancy of Cr at the Al octahedral site. The synthetic material was dehydrated at 800°C for 4 h, yielding a sample with less than 0.3 molecules of H_2O per formula unit.

Crystals of natural euclase from Minas Gerais, Brazil (National Museum of Natural History, Smithsonian Institution, specimen no. #121350), were provided by John White. Chemical analysis of this colorless, gem-quality material by Barton (1986) showed no impurities. Crystal fragments of dimensions approximately 100 × 100 × 40 μm were used for X-ray diffraction studies at room and high pressure.

Data collection at room pressure

Room-temperature lattice parameters for both minerals were refined from diffractometer angles of twenty reflections, each of which was measured in eight equivalent positions, by the method of King and Finger (1979). Unit-cell parameters refined without symmetry constraints (i.e., as triclinic) are consistent with hexagonal and monoclinic symmetry, respectively, for beryl and euclase (Table 1).

Intensities of all reflections in a hemisphere with $(\sin\theta)/\lambda \leqq 0.7$ were measured by an automated, four-circle diffractometer with graphite monochromatized Mo$K\alpha$ radiation. Omega step scans with 0.025° step increments and 4-s counting time per step were used. Digitized data were converted to graphical form, and integrated peak intensities were determined by the method of Lehmann and Larsen (1974) with an option for manual intervention. Refinement conditions and refined structural parameters for beryl and euclase appear in Tables 2 and 3, respectively. Refined anisotropic temperature parameters and the magnitudes and orientation of thermal vibration ellipsoids for both minerals at room conditions appear in Tables 4 and 5.[1]

Data collection at high pressure

Flat, platelike crystals approximately 40 μm thick were mounted in a diamond-anvil pressure cell for X-ray diffraction, with an alcohol mixture of 4:1 methanol : ethanol as the hydrostatic pressure medium and 5–10-μm chips of ruby as the internal pressure calibrant. Pressure-cell design, loading, operation, and calibration were as described by Hazen and Finger (1982). Special care was taken to avoid X-ray shielding by the gasket parts of the diamond cell. Large gasket holes of 400 μm were used, and the 100 μm crystals were well centered in the diamond cell throughout the experiments.

Lattice constants of the two Be aluminosilicates were determined at several pressures. From 12 to 20 reflections were measured by the method of Hamilton (1974), as modified by King and Finger (1979), in order to correct for errors in crystal centering on the diffractometer as well as diffractometer alignment. Each set of angular data was refined without constraint, and the resultant "triclinic" cell was examined for conformity with expected hexagonal and monoclinic symmetries of beryl and euclase, respectively. These symmetry conditions were met within two standard deviations at all pressures studied. High-pressure unit-cell parameters are recorded in Table 1.

[1] To obtain copies of Tables 4, 5, and 6a to 6h, order Document AM-86-310 from the Business Office, Mineralogical Society of America, 1625 I Street, N.W., Suite 414, Washington, D.C. 20006. Please remit $5.00 in advance for the microfiche.

Table 3. Euclase refinement conditions and refined atomic parameters

		1 bar	21 kbar	42 kbar	62 kbar
Number of Obs. ($I>2\sigma$)		745	204	191	197
R (%)+		4.1	4.2	4.8	4.0
Weighted R (%)+		2.6	3.3	3.8	3.2
Extinction r* (x10⁵)		3.7(3)*	7.2(8)	6.4(8)	3.2(5)
Atom	Parameter				
Si	x	0.17752(13)	0.1784(4)	0.1784(5)	0.1793(3)
	y	0.10027(5)	0.1002(4)	0.1007(5)	0.1002(4)
	z	0.53639(14)	0.5359(4)	0.5364(5)	0.5359(4)
	B	0.39(1)	0.58(5)	0.74(6)	0.64(5)
Al	x	0.24877(14)	0.2477(4)	0.2481(5)	0.2481(4)
	y	0.44470(5)	0.4441(4)	0.4433(6)	0.4428(4)
	z	0.95708(15)	0.9576(4)	0.9573(5)	0.9582(4)
	B	0.45(1)	0.70(5)	0.80(6)	0.68(5)
Be	x	0.1741(6)	0.1707(19)	0.1697(21)	0.1719(16)
	y	0.3006(2)	0.2985(20)	0.3038(24)	0.3029(18)
	z	0.4571(7)	0.4573(19)	0.4550(22)	0.4524(19)
	B	0.60(5)*	1.0(2)	0.9(2)	0.9(2)
O1	x	0.3818(3)	0.3831(9)	0.3818(10)	0.3840(8)
	y	0.0324(1)	0.0324(8)	0.0323(10)	0.0320(8)
	z	0.7630(3)	0.7592(9)	0.7611(11)	0.7609(9)
	B	0.52(3)	0.69(10)	0.01(12)	0.94(10)
O2	x	0.3800(3)	0.3790(10)	0.3754(11)	0.3758(8)
	y	0.3770(1)	0.3772(8)	0.3783(10)	0.3780(8)
	z	0.6521(3)	0.6489(9)	0.6487(11)	0.6484(9)
	B	0.50(3)	0.67(9)	0.76(12)	0.75(9)
O3	x	0.3431(3)	0.3445(9)	0.3439(10)	0.3463(8)
	y	0.1998(1)	0.1966(9)	0.1984(11)	0.1990(9)
	z	0.5248(6)	0.5291(9)	0.5303(10)	0.5313(9)
	B	0.53(3)	0.65(10)	0.67(11)	0.65(9)
O4	x	0.1006(3)	0.1010(8)	0.1031(10)	0.1042(8)
	y	0.0531(1)	0.0542(9)	0.0543(11)	0.0563(8)
	z	0.2113(3)	0.2096(8)	0.2101(10)	0.2074(8)
	B	0.50(3)	0.67(9)	0.79(11)	0.70(9)
O5	x	0.1596(4)	0.1586(9)	0.1562(11)	0.1558(8)
	y	0.3320(1)	0.3297(8)	0.3295(10)	0.3256(7)
	z	0.1206(4)	0.1156(9)	0.1175(11)	0.1144(9)
	B	0.71(3)	0.81(10)	0.91(12)	0.74(9)
H	x	0.063(9)	Not Refined		
	y	0.302(3)			
	z	0.011(9)			
	B	2.4(10)			

* Parenthesized figures represent esd's.

+ $R = \Sigma[|F_o| - |F_c|]/\Sigma F_o$

Weighted $R = [\Sigma_w(|F_o| - |F_c|)^2/\Sigma w F_o^2]^{1/2}$

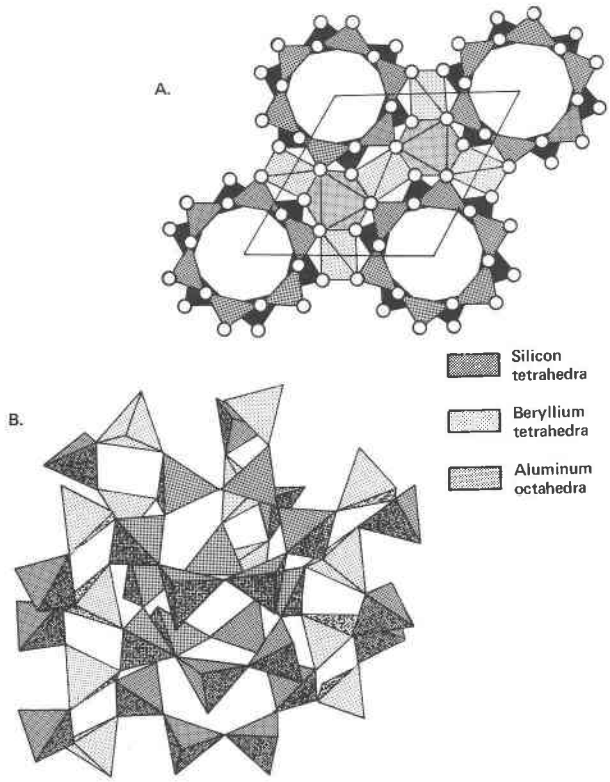

Fig. 1. The crystal structure of beryl (after Gibbs et al., 1968). (A) The c-axis projection shows the six-member tetrahedral rings of Si, which are cross-linked by Be tetrahedra and Al octahedra. (B) The arrangement of Si and Be tetrahedra results in a continuous three-dimensional framework.

Intensity data for three-dimensional structure refinements were collected on all reflections accessible within the region $(\sin\theta)/\lambda \leqq 0.7$. Omega increments of 0.02° and long counting times of 8 to 10 s per increment were used to optimize the number of observed reflections and the precision of the intensities. Observed and calculated structure factors at four pressures for both beryl and euclase are recorded in Tables 6a to 6h (see footnote 1). The fixed-ϕ mode of data collection (Finger and King, 1978) was used to maximize reflection accessibility and minimize attenuation by the diamond cell, and corrections were made for Lorentz and polarization effects, crystal absorption and X-ray absorption by the diamond and Be components of the pressure cell (Hazen and Finger, 1982). Conditions of high-pressure refinements, refined isotropic extinction coefficients (Zachariasen, 1967), atomic positional parameters, and isotropic thermal parameters are recorded in Tables 2 and 3.

Results

Room-pressure refinements

Refined atomic coordinates of beryl are in close agreement with those of Gibbs et al. (1968) and Morosin (1972). The four Si–O bonds in the Si tetrahedron (point symmetry *m*) range from 1.595 to 1.619 Å, with an average value of 1.608 Å (Table 7). The Si tetrahedron is nearly regular, with O–Si–O angles deviating by no more than 1.5° from the ideal 109.5° tetrahedral angle. All six Al–O bonds in the Al octahedron (point symmetry 32) are symmetrically equivalent, with length 1.908 Å; however, this polyhedron is significantly elongated parallel to **c**, with O–Al–O angles ranging from 76.5 to 96.8°.

The beryl Be tetrahedron (point symmetry 222) is one of the most distorted cation polyhedra in any Be mineral (Table 8), with a quadratic elongation of 1.09 and an angle variance of 327 (Hazen and Finger, 1982). All Be–O bonds are symmetrically equivalent (1.657 Å), but O–Be–O angles range from 91 to 131° compared to the ideal 109.5° value. The resulting tetrahedron is both flattened and elongated in the (001) plane. These distortions may be explained, in part, by the shortened shared edges between Be and Al polyhedra (Gibbs et al., 1968).

Anisotropic temperature factors of beryl atoms are in qualitative agreement with those reported by Morosin (1972), though absolute values of isotropic and anisotropic thermal parameters are somewhat larger than in previous studies. Extinction (Table 2), which is a large

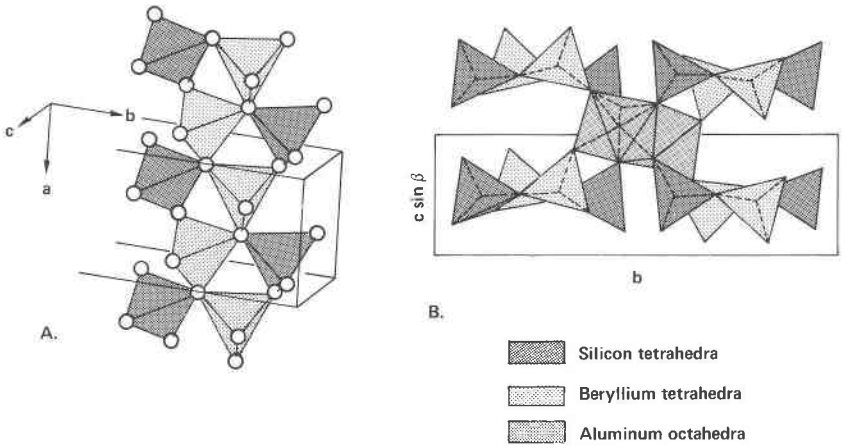

Fig. 2. The crystal structure of euclase. (A) The double tetrahedral strip parallel to **a** (after Mrose and Appleman, 1962). (B) The **a**-axis projection shows cross-linkages of Be and Si tetrahedral chains by Al octahedra.

effect in most Be minerals and which is inversely correlated with thermal parameters, may contribute to these differences. The O1 oxygen, which links adjacent tetrahedra in the six-member ring, displays the largest thermal anisotropy. Its motion is described by a flattened spheroid with major axes perpendicular to the Si–O–Si direction.

Refined positional parameters of euclase are identical within estimated errors to those reported by Mrose and Appleman (1962). Euclase Be and Si tetrahedra (both with point symmetry 1) are nearly regular (Table 8), with mean Si–O and Be–O distances of 1.633 and 1.643 Å, respectively (Table 9). The Al octahedron (point symmetry 1) is less regular, with Al–O distances from 1.85 to 1.99 Å (mean 1.903 Å), and O–Al–O angles from 79.8 to 99.3°.

Table 7. Beryl selected bond distances and angles

Bond/Angle	1 bar	18 kbar	36 kbar	57 kbar
Be-O2 [4]+	1.657(1)*	1.654(3)	1.644(3)	1.626(4)
O2-Be-O2 [2]	91.0(1)	90.9(3)	91.3(2)	90.2(3)
O2-Be-O2 [2]	109.0(1)	108.9(3)	108.5(3)	109.7(3)
O2-Be-O2 [2]	131.2(1)	131.3(2)	131.3(3)	131.4(3)
Al-O2 [6]	1.908(1)	1.900(4)	1.900(4)	1.882(5)
O2-Al-O2 [6]	96.8(1)	96.6(2)	96.7(2)	97.4(2)
O2-Al-O2 [3]	90.6(1)	90.7(2)	90.9(2)	90.6(3)
O2-Al-O2 [3]	76.5(1)	76.7(2)	76.4(2)	75.5(3)
Si-O1	1.595(2)	1.589(5)	1.584(5)	1.583(7)
Si-O1	1.597(2)	1.595(5)	1.592(4)	1.596(6)
Si-O2 [2]	1.619(1)	1.608(4)	1.600(4)	1.613(5)
Mean Si-O	1.608	1.600	1.594	1.601
O1-Si-O1	108.4(2)	109.0(4)	108.4(4)	107.7(5)
O1-Si-O2 [2]	108.4(1)	108.4(2)	108.2(2)	108.1(2)
O1-Si-O2 [2]	110.3(1)	109.8(2)	110.4(2)	110.4(2)
O2-Si-O2	111.1(1)	111.3(3)	111.1(3)	112.0(4)
O1-Si	1.595(2)	1.589(5)	1.584(5)	1.583(7)
O1-Si	1.597(2)	1.595(5)	1.592(4)	1.596(6)
Si-O1-Si	168.4(2)	169.0(4)	168.4(4)	167.7
O2-Be	1.657(1)	1.654(3)	1.644(3)	1.626(4)
O2-Al	1.908(1)	1.900(4)	1.900(4)	1.882(5)
O2-Si	1.619(1)	1.608(4)	1.600(4)	1.613(5)
Be-O2-Al	96.3(1)	96.2(2)	96.1(2)	97.2(2)
Be-O2-Si	127.0(1)	126.8(2)	127.4(2)	127.0(3)
Al-O2-Si	136.7(1)	137.0(2)	136.4(2)	135.7(3)

* Parenthesized figures represent esd's.

\+ Bracketed figures represent bond and angle multiplicities.

The shortest octahedral O–O distance corresponds to the shared edge between Al octahedra.

A three-dimensional difference Fourier synthesis showed no significant features except for a maximum near the O5 (hydroxyl) position, which was refined as H. This position is consistent with that found by Hanisch and Zemann (1966) from infrared pleochroism. The H atom lies near the Al–O5–Be plane, with an O–H distance of 0.76 Å.

The anions with the greatest thermal vibration anisotropies are planar three-coordinated O2, O3, and O5, which have maximum vibration amplitude perpendicular to the planes of cation–anion bonding.

Linear compressibilities and bulk moduli

Unit-cell parameters at several pressures (Table 1) were used to calculate linear compressibilities and pressure-volume equation-of-state parameters. Unit-cell edges and the β angle of euclase were described with the expression

$$a = a_0 - d_1P + d_2P^2,$$

where a_0 is the value of the cell parameter at room pressure, and d_1 and d_2 are fitted parameters. The d_2 parameters are not significant for any of the parameters in beryl and euclase.

Beryl compressibility (Table 10) is nearly isotropic, with the c axis approximately 20% more compressible than a, and a corresponding small decrease in c/a with increasing pressure (Table 1). Monoclinic euclase (Table 10), on the other hand, is characterized by significant compression anisotropy, which is best represented by a strain ellipsoid (Hazen and Finger, 1982). One axis of the ellipsoid is constrained by symmetry to coincide with the b axis, but the other two principal axes need lie only in the **a**-**c** plane. The compression strain ellipsoid for euclase was determined with program STRAIN (Ohashi, 1982). Maximum compression ($2.44 \pm 0.05 \times 10^{-4}$ kbar^{-1}) is parallel to the **b** axis, whereas the axis of minimum compressibility ($1.50 \pm 0.03 \times 10^{-4}$ kbar^{-1}) is approximately 35° from **a**, near [101]. Note that this minimum compression axis is

thus subparallel to the tetrahedral chain, which is composed of rigid Be–Be–Si three-member rings. The axis of intermediate compression ($1.96 \pm 0.05 \times 10^{-4}$ kbar^{-1}) lies in the **a**-**c** plane at right angles to the major and minor ellipsoid axes. Axial compression ratios for euclase are 1.00:1.24:1.63.

Pressure-volume equation-of-state parameters, bulk modulus K for both minerals and the pressure derivative of the bulk modulus K' for euclase were calculated by least-squares fit of unit-cell volume data to a Birch-Murnaghan equation. The pressure derivative K' of beryl was constrained to be 3.9, based on the elasticity measurements of Yoon and Newnham (1973). The bulk modulus calculated from the present X-ray studies is 1.70 ± 0.05 Mbar, in reasonable agreement with the 1.80-Mbar modulus determined by Yoon and Newnham. Conversely, if the bulk modulus is constrained to Yoon and Newnham's value of 1.8 Mbar, then K' based on the present data is -2 ± 6.

The bulk modulus of euclase is 1.59 ± 0.03 Mbar if the pressure derivative of the bulk modulus K' is assumed to be 4. A second-order equation, alternatively, gives 1.5 ± 0.2 Mbar and 9 ± 5 for the euclase bulk modulus and its pressure derivative, respectively.

Swanson et al. (1985) demonstrated that unit-cell parameters measured on a single-crystal diffractometer may vary systematically with the range of θ; cell parameters determined from low-angle reflections, including those of beryl in the present study, are as much as 0.1% smaller than those determined from high-angle data. Thus, it is essential to use unit-cell parameters from one range of θ when employing X-ray data for equation-of-state studies. All of the pressure-volume data used in the beryl and euclase equation-of-state results noted above were measured from reflections with $2\theta \approx 25°$. If, however, the beryl data are supplemented by a room-pressure unit cell determined with 45 to 55° reflections and a 54-kbar unit cell determined by 14° reflections (Table 1), the resultant beryl bulk modulus is 1.47 ± 0.05 Mbar, a value that is more than four standard deviations below the 1.7-Mbar modulus derived from 25° reflections only. Unit-cell parameters of crystals at room pressure are usually determined from higher-angle X-ray data than unit cells at high pressure. Bulk moduli calculated from such "mixed" diffraction data may thus be systematically low, compared to bulk moduli determined by ultrasonic or Brillouin scattering techniques. Care should be taken in future high-pressure and high-temperature studies to obtain unit-cell constants from the same range of 2θ at all conditions.

High-pressure crystal structure of beryl

Beryl is composed of three symmetrically and chemically distinct polyhedra—tetrahedra of Si and Be and an octahedron of Al—all of which undergo significant compression from 1 bar to 47 kbar. Polyhedral bulk moduli, calculated from changes in volumes of enclosure defined by oxygen positions surrounding each cation (Table 8), are 1.4 ± 0.4, 2.3 ± 0.6, and 1.4 ± 0.5 Mbar for Be, Si, and Al, respectively. Polyhedral distortions, as characterized by quadratic elongation and bond angle variance (Table 8; Robinson et al., 1971) do not vary significantly with changing pressure.

Table 8. Polyhedral volumes (Å^3) and distortion parameters for beryl and euclase at several pressures

BERYL					
Atom		1 bar	19 kbar	36 kbar	47 kbar
Si	Vol	2.127(4)	2.100(9)	2.072(9)	2.105(12)
	QE+	1.001(2)	1.000(4)	1.001(4)	1.001(5)
	AV‡	1.7	1.4	2.1	3.2
Be	Vol	2.041(3)	2.030(7)	1.995(8)	1.921(8)
	QE	1.093(1)	1.094(3)	1.093(4)	1.097(4)
	AV	327	330	324	342
Al	Vol	8.953(8)	8.867(20)	8.834(25)	8.559(24)
	QE	1.022(1)	1.021(2)	1.021(3)	1.025(3)
	AV	74	72	74	87

EUCLASE					
Atom		1 bar	21 kbar	41 kbar	62 kbar
Si	Vol	2.23(1)	2.15(2)	2.16(2)	2.15(2)
	QE	1.001(1)	1.002(2)	1.001(5)	1.002(5)
	AV	4	6	5	6
Al	Vol	9.045(8)	9.04(4)	8.94(4)	8.89(4)
	QE	1.011(2)	1.012(9)	1.012(11)	1.012(11)
	AV	38	37	39	39
Be	Vol	2.258(4)	2.28(3)	2.23(3)	2.20(3)
	QE	1.005(3)	1.01(2)	1.00(2)	1.00(2)
	AV	16	21	12	11

+QE = Quadratic elongation = $\sum_{i=1}^{n}[(\ell_i/\ell_o)^2/n]$

‡ AV = Angle variance = $\sum_{i=1}^{n}[(\theta_i - \theta_o)^2/(n-1)]$

Crystal compression in silicates can be described as a combination of polyhedral compression and changes in interpolyhedral angles (Hazen and Finger, 1985). Cation–oxygen–cation angles in beryl are constant. The O2 oxygen is in planar three-coordination, and it remains in the Be–Al–Si plane throughout the pressure range of this study. The O1 oxygen links Si tetrahedra in the six-member rings, which have hexagonal symmetry, thus restricting Si–O–Si bending. Note, however, that if the beryl structure distorts to a trigonal, orthorhombic, or lower-symmetry form at higher pressure, then unrestricted Si–O–Si bending may become an important compression mechanism.

The unit-cell anisotropy of beryl, in which the c axis is 20% more compressible than a, probably reflects the relative compressibility of the three different polyhedral units. Si tetrahedra are the least-compressible elements, so that the (001) plane of the rigid Si_6O_{18} rings is less compressible than the c axis, which can be shortened by compression of Be and Al octahedra alone. Note, however, that the bulk moduli of all three polyhedra are within one estimated standard deviation of the 1.7-Mbar crystal modulus, so the slight compression anisotropy cannot be ascribed unequivocally to any one structural unit.

Table 9. Euclase selected bond distances and angles

Bond/Angle	1 bar	21 kbar	42 kbar	62 kbar
Silicon tetrahedron				
Si-O1	1.623(2)	1.608(8)	1.609(10)	1.605(8)
Si-O2	1.640(2)	1.634(5)	1.639(6)	1.638(5)
Si-O3	1.637(2)	1.589(12)	1.596(16)	1.607(12)
Si-O4	1.632(2)	1.623(7)	1.620(9)	1.608(6)
Mean Si-O	1.633	1.614	1.616	1.615
O1-Si-O2	111.3(1)	112.2(3)	111.6(4)	112.0(3)
O1-Si-O3	107.7(1)	106.6(4)	107.1(5)	106.7(4)
O1-Si-O4	111.0(1)	111.3(6)	111.0(7)	112.2(5)
O2-Si-O3	106.9(1)	107.5(6)	108.0(7)	107.5(5)
O2-Si-O4	108.6(1)	108.0(3)	107.7(3)	107.8(2)
O3-Si-O4	111.2(1)	111.3(4)	111.5(5)	110.5(4)
Aluminum Octahedron				
Al-O1	1.852(2)	1.843(5)	1.844(6)	1.833(5)
Al-O1	1.985(2)	1.991(9)	1.983(12)	1.980(8)
Al-O2	1.910(2)	1.909(8)	1.880(9)	1.876(7)
Al-O4	1.873(2)	1.867(4)	1.871(5)	1.861(4)
Al-O4	1.934(2)	1.942(12)	1.940(15)	1.956(10)
Al-O5	1.866(2)	1.866(12)	1.858(14)	1.849(10)
Mean Al-O	1.903	1.903	1.896	1.893
Beryllium Tetrahedron				
Be-O2	1.633(3)	1.646(22)	1.599(26)	1.599(19)
Be-O3	1.658(3)	1.645(10)	1.644(11)	1.643(9)
Be-O3	1.667(3)	1.675(10)	1.714(35)	1.693(26)
Be-O5	1.612(4)	1.628(12)	1.585(13)	1.579(11)
Mean Be-O	1.643	1.644	1.634	1.629
O2-Be-O3	104.8(2)	104.8(6)	103.8(7)	103.5(12)
O2-Be-O3	113.4(2)	111.3(12)	113.6(13)	112.5(9)
O2-Be-O5	105.4(2)	104.3(13)	108.0(16)	108.6(12)
O3-Be-O3	114.1(2)	116.6(14)	112.2(16)	112.3(12)
O3-Be-O5	107.8(2)	108.1(7)	109.5(7)	109.6(6)
O3-Be-O5	111.2(2)	111.1(10)	109.5(13)	110.2(10)
O1 (3-coordinated)				
O1-Si	1.623(2)	1.608(8)	1.609(10)	1.605(8)
O1-Al	1.852(2)	1.843(5)	1.844(6)	1.833(5)
O1-Al	1.985(2)	1.991(9)	1.983(11)	1.980(0)

Bond/Angle	1 bar	21 kbar	42 kbar	62 kbar
O1 (continued)				
Al-O1-Al	100.2(1)	99.5(3)	100.1(4)	100.4(3)
Al-O1-Si	125.4(1)	125.1(3)	125.7(3)	125.2(2)
Al-O1-Si	128.0(1)	128.3(7)	127.4(8)	127.4(6)
O2 (3-coordinated)				
O2-Si	1.640(2)	1.646(22)	1.639(6)	1.638(5)
O2-Al	1.910(2)	1.909(8)	1.880(9)	1.876(7)
O2-Be	1.633(3)	1.634(5)	1.599(26)	1.599(19)
Si-O2-Al	124.1(1)	124.0(6)	124.5(7)	124.2(5)
Si-O2-Be	115.1(1)	116.1(5)	115.3(6)	115.1(5)
Al-O2-Be	120.3(1)	119.7(4)	119.9(5)	120.4(4)
O3 (3-coordinated)				
O3-Si	1.637(2)	1.589(12)	1.596(16)	1.607(12)
O3-Be	1.658(3)	1.645(10)	1.644(11)	1.643(9)
O3-Be	1.667(3)	1.675(28)	1.714(35)	1.693(26)
Si-O3-Be	122.9(1)	122.1(11)	122.7(7)	122.4(5)
Si-O3-Be	119.0(1)	121.6(6)	118.1(14)	118.1(10)
Be-O3-Be	114.5(1)	112.0(9)	114.4(10)	114.1(7)
O4 (3-coordinated)				
O4-Si	1.632(2)	1.623(7)	1.620(9)	1.608(6)
O4-Al	1.873(2)	1.867(4)	1.871(5)	1.861(4)
O4-Al	1.934(2)	1.942(12)	1.940(14)	1.956(10)
Si-O4-Al	131.8(1)	131.0(5)	131.4(6)	130.7(4)
Si-O4-Al	127.0(1)	127.1(5)	126.5(6)	126.7(4)
Al-O4-Al	96.7(1)	96.9(4)	96.9(5)	96.6(4)
O5 (3-coordinated)				
O5-Al	1.866(2)	1.866(12)	1.858(14)	1.849(10)
O5-Be	1.612(4)	1.628(12)	1.585(13)	1.579(11)
O5-H	0.76(4)	-	-	-
Al-O5-Be	131.4(2)	130.2(11)	128.1(14)	127.3(10)
Al-O5-H	114(3)			
Be-O5-H	112(3)			

* Parenthesized figures represent esd's.

High-pressure crystal structure of euclase

The three cation polyhedra that are found in beryl also form the euclase structure. All three polyhedral bulk moduli in euclase are approximately 2.3 ± 0.7 Mbar. The relatively large percentage errors on these and other polyhedral bulk moduli in Be silicates are a consequence of the difficulties inherent in detecting subtle shifts of low-Z cation and oxygen positions as a function of pressure. Note that polyhedral distortion indices (Table 8) do not vary significantly with pressure. The 2.3-Mbar polyhedral moduli correspond to a linear compressibility of about 1.5×10^{-4} kbar^{-1}. This value is identical to that of the minimum compression axis of euclase in the **a-c** plane and indicates that structural changes in this direction are controlled by changes in polyhedral volumes. The significantly greater compressibility of euclase perpendicular to this direction is a consequence of cation–oxygen–cation bond bending.

Table 10. Axial compressibilities of beryl and euclase

BERYL	
$a = 9.028\pm0.001 - 0.00158\pm0.00003P$	($\beta_{\perp} = 1.72\pm0.04\times10^{-4}$ kbar^{-1})
$c = 9.188\pm0.003 - 0.00193\pm0.00007P$	($\beta_{/\!/} = 2.10\pm0.09\times10^{-4}$ kbar^{-1})
EUCLASE	
$a = 4.7797\pm0.0007 - 0.00082\pm0.00003P$	($\beta_a = 1.72\pm0.06\times10^{-4}$ kbar^{-1})
$b = 14.332\pm0.001 - 0.00350\pm0.00007P$	($\beta_b = 2.44\pm0.05\times10^{-4}$ kbar^{-1})
$c = 4.6334\pm0.0006 - 0.00088\pm0.00003P$	($\beta_c = 1.91\pm0.06\times10^{-4}$ kbar^{-1})
$\beta = 100.32\pm0.02 - 0.0032\pm0.0006P$	

Axes a, b, and c are unit-cell edge lengths in Å and β is the unit-cell angle of euclase in degrees, whereas β's with subscripts represent linear compressibilities. Pressure is in kbar.

The effects of changing interpolyhedral angles may be analyzed by first considering separately the chains of tetrahedra and octahedra parallel to **a**, and then examining the cross-linkages of these chains. There are four symmetrically distinct T–O–T angles in the tetrahedral strip, three involving O3 and one involving O2. All of these angles are unchanged between 1 bar and 62 kbar, so the tetrahedral strip is a relatively rigid structural unit. Two different Al–O–Al angles occur in the Al octahedral strips, and these angles are also unchanged with pressure. However, cation–oxygen–cation angles that link tetrahedral and octahedral strips all undergo some decrease with increasing pressure, particularly the Al–O4–Si angle, which changes from 132 to 130°, and the Al–O5–Be angle, which decreases from 131 to 127°. These significant changes in interpolyhedral angles result in the observed anisotropic compression of the euclase unit cell.

Discussion

Comparison of beryl and euclase with Be orthosilicates at high pressure

Hazen and Au (1986) have described high-pressure structure data for phenakite (Be_2SiO_4) and bertrandite

[$Be_4Si_2O_7(OH)$], which may be represented by continuous, three-dimensional frameworks of Be and Si tetrahedra. Polyhedral bulk moduli in these two orthosilicates are similar to those recorded here for beryl and euclase. All four symmetrically distinct Be tetrahedra in phenakite and bertrandite have bulk moduli of approximately 2 Mbar, which is the same value observed in bromellite (BeO). The 2.3 ± 0.7 Mbar Be tetrahedral modulus in euclase is consistent with this value, although the 1.4 ± 0.4 Mbar modulus of beryl's very distorted Be tetrahedron is slightly lower than other observed values.

Si tetrahedral bulk moduli in beryl and euclase are both greater than 2 Mbar, consistent with the 2.7 ± 0.4 and 1.8 ± 0.5 Mbar values for phenakite and bertrandite, respectively. With the exception of the distorted Be tetrahedron in beryl, all Be, Al, and Si polyhedra in these minerals from the system BeO-Al_2O_3-SiO_2-H_2O have bulk moduli consistent with 2 Mbar or greater. These polyhedra are significantly less compressible than monovalent or divalent cations in six or greater coordination (Hazen and Finger, 1982).

It is evident from the several Be silicates that compression anisotropies are closely related to polyhedral linkages. The most rigid structural element in these minerals is the three-member Be–Be–Si ring, which occurs in phenakite, bertrandite, and euclase. These rings do not bend with increasing pressure, and their compressibility is thus that of the constituent polyhedra—approximately 2 Mbar (corresponding to a linear compressibility of about 1.6×10^{-4} $kbar^{-1}$). These three-member rings control compression along the phenakite **c** axis and the euclase **a** axis. Four-member rings of two Be and two Si tetrahedra occur in phenakite, bertrandite, and beryl; they are also relatively rigid, limiting compression in the (001) planes of hexagonal phenakite and beryl. Six-member tetrahedral rings with hexagonal symmetry, as in phenakite and beryl, also do not deform, acting as rigid structural units. Significant compression occurs in Be silicates only when angles between adjacent corner-linked polyhedra are free to bend. This situation occurs in both bertrandite and euclase, which are the most compressible of the Be minerals studied.

High-temperature versus high-pressure behavior of beryl

Morosin (1972) determined thermal expansion coefficients for beryl from −200 to 800°C. The *c* axis undergoes moderate expansion of about 2×10^{-6} $°C^{-1}$, whereas the *a* axis shows only slight expansion over this range and actually contracts with increasing temperature below about 200°C. At first sight, this extreme anisotropy in beryl thermal expansion might seem inconsistent with the relatively isotropic compression behavior. However, the expansion anisotropy is not surprising considering the very different thermal expansion behavior of Be and Si tetrahedra, as opposed to the very similar compression behavior. In all silicate structures determined at high temperatures, the Si tetrahedral volume is unchanged with increasing temperature. Furthermore, rigid groups of Si tetrahedra such as the six-member ring in beryl often display thermal contraction as a result of increased bridging-oxygen vibration amplitudes while Si–O distances remain constant (Hazen and Finger, 1982). Be tetrahedra, on the other hand, are expected to undergo a moderate linear expansion of about 10^{-5} $°C^{-1}$, on the basis of the observed relationship between bond thermal expansion and Pauling bond strength (Hazen and Finger, 1982). In the (001) plane in beryl, thermal expansion is constrained by the "shrinking" Si tetrahedral rings, but modest expansion is possible parallel to **c** because of the expansion of Be tetrahedra. Work now in progress on Be silicate structures at high temperature should clarify the relative magnitudes of polyhedral thermal expansion in these minerals.

Elasticity of beryl and euclase

Yoon and Newnham (1973) reported single-crystal elastic stiffnesses of beryl. They observed small compression anisotropies, similar to those determined in this study, with $\beta_\perp > \beta_\parallel$. Newnham and Yoon (1973) presented a simple mechanical model to rationalize observed compressional stiffnesses in beryl and other silicates on the basis of structural geometry. They observed that the least-compressible directions generally conform to directions of linked Si tetrahedra. Axes of tetrahedral chains in amphiboles and pyroxenes and planes of tetrahedral sheets and rings in layer silicates and beryl are thus expected to be the least-compressible directions in these minerals.

Be tetrahedra and Al octahedra are, on average, only slightly more compressible than Si tetrahedra in the Be aluminosilicates studied, and one must consider the complete Be-Al-Si polyhedral framework, therefore, when applying a structural model such as that of Newnham and Yoon. The *c*-axis compression of beryl, for example, is only 20% greater than that of the *a* axis, in spite of the planar configuration of rigid Si tetrahedra. The three-dimensional polyhedral framework (Fig. 1) gives the structure rigidity along both **a** and **c**. In euclase the Si tetrahedra are not linked to each other, and no axis of minimum compression can be inferred by consideration of Si tetrahedra alone. Recognition of the Be-Si tetrahedral chains (Fig. 2a) and cross-linking octahedral chains (Fig. 2b) as rigid structural elements is the key to understanding the anisotropic compression of euclase.

Although the mechanical model of Newnham and Yoon was applied only to compressional moduli, a similar approach may be used to rationalize shear moduli on the basis of structure (e.g., Vaughan and Weidner, 1978; Levien et al., 1980; Weidner and Vaughan, 1982; Bass and Weidner, 1984). Three-member rings of tetrahedra, such as the Be–Be–Si rings common to many Be silicates, behave as rigid structural units that are difficult to deform. When these rings form continuous strips or layers, as in phenakite or euclase, then unusually large shear moduli occur in the associated planes. The C_{44} elastic stiffness coefficient of phenakite (corresponding to pure shear in the **a**-**c** plane of the hexagonal mineral) is approximately 1 Mbar, compared with the 0.6-Mbar stiffnesses typical

of shear moduli in beryl. A similar large shear stiffness should be associated with the **a-b** plane of euclase because of the rigid tetrahedral chains lying in this plane. (The elastic moduli of euclase have not been determined.)

Shearing in Be silicates should be particularly easy in planes with interpolyhedral angles that are free to bend. Observed changes in angles between tetrahedral and octahedral strips of euclase at high pressure suggest that shear stiffnesses associated with the **b-c** plane will be unusually small. Let C_{11}, C_{22}, and C_{33} represent euclase elastic moduli of pure compression in the **a**, **b**, and **c*** directions, respectively. It follows from compressibility observations of the present study that $C_{22} > C_{33} > C_{11}$. On the basis of the structural arrangement of rigid Be–Be–Si tetrahedral rings and flexible interpolyhedral angles, we predict that $C_{66} > C_{55} > C_{44}$ (the pure shear stiffnesses associated with the **a-b**, **a-c***, and **b-c*** planes, respectively). Hence, euclase should have shear as well as compressional anisotropies.

Summary

Polyhedral properties, including size, shape, compressibility, thermal expansivity, and elastic character, are similar for a given type of polyhedron in different structures. Thus the Be tetrahedral bulk modulus is approximately 2 Mbar in bromellite, phenakite, chrysoberyl, bertrandite, and euclase. Only in beryl, with a severely distorted Be tetrahedron, is a smaller Be polyhedral bulk modulus observed.

Studies of Be silicates have also shown that groups of polyhedra, such as the three-member Be–Be–Si tetrahedral ring, may behave similarly from structure to structure. Compression anisotropies and shear moduli of several Be minerals seem to be controlled by the distribution of these rings. These arguments thus provide a practical and intuitive method to relate mineral structures and physical properties. Further experiments now in progress on the structures and properties of minerals in the system BeO-Al_2O_3-SiO_2-H_2O, combined with ab initio molecular orbital calculations on characteristic Be-Al-Si polyhedral clusters, will help to define the potential and limitations of the polyhedral approach.

Acknowledgments

The authors gratefully acknowledge the constructive reviews of F. Chayes, J. W. Downs, F. C. Hawthorne, R. E. Newnham, and H. S. Yoder, Jr. This research was supported in part by National Science Foundation grants EAR83-19209 and EAR84-19982.

References

Au, A.Y., and Hazen, R.M. (1985) Polyhedral modeling of the elastic properties of corundum (α-Al_2O_3) and chrysoberyl (Al_2BeO_4). Geophysical Research Letters, 12, 725–728.

Barton, M.D. (1986) Phase equilibria and thermodynamic properties of minerals in the BeO-Al_2O_3-SiO_2-H_2O (BASH) system, with petrologic applications. American Mineralogist, 71, 277–300.

Bass, J.D., and Weidner, D.J. (1984) Elasticity of single-crystal orthoferrosilite. Journal of Geophysical Research, 89, 4359–4371.

Finger, L.W., and King, H.E. (1978) A revised method of operation of the single-crystal diamond cell and refinement of the structure of NaCl at 32 kbar. American Mineralogist, 63, 337–342.

Gibbs, G.V., Breck, D.W., and Meagher, E.P. (1968) Structural refinement of hydrous and anhydrous synthetic beryl, $Al_2Be_3Si_6O_{18}$ and emerald, $Al_{1.9}Cr_{0.1}Be_3Si_6O_{18}$. Lithos, 1, 275–285.

Hamilton, W.C. (1974) Angle settings for four-circle diffractometers. In International tables for X-ray crystallography, 4, 273–284. Kynoch Press, Birmingham, England.

Hanisch, K., and Zemann, J. (1966) Messung des Ultrarot-Pleochroismus von Mineralen. VII. Der Pleochroismus der OH-Streckfrequenz in Euklas. Neus Jahrbuch für Mineralogie, Monatshefte 1966, 346–348.

Hazen, R.M. (1985) Comparative crystal chemistry and the polyhedral approach. Reviews in Mineralogy, 14, 317–346.

Hazen, R.M., and Au, A.Y. (1986) High-pressure crystal chemistry of phenakite (Be_2SiO_4) and bertrandite ($Be_4Si_2O_7(OH)_2$). Physics and Chemistry of Minerals, 13, 69–78.

Hazen, R.M., and Finger, L.W. (1982) Comparative crystal chemistry. Wiley, New York.

——— (1985) Crystals at high pressure. Scientific American, 252, 110–117.

Hoering, T.C., and Hofmeister, A.M. (1985) Spectroscopic modeling of C_v for Be-Al-Si minerals. (abs.) EOS (American Geophysical Union Transactions), 66, 357.

King, H.E., and Finger, L.W. (1979) Diffracted beam crystal centering and its application to high-pressure crystallography. Journal of Applied Crystallography, 12, 374–378.

Lehmann, M.S., and Larsen, F.K. (1974) A method for location of the peaks in step-scan-measured Bragg reflections. Acta Crystallographica, A30, 580–584.

Levien, L., Prewitt, C.T., and Weidner, D.J. (1980) Structure and elastic properties of quartz at pressure. American Mineralogist, 65, 920–930.

Morosin, Bruno. (1972) Structure and thermal expansion of beryl. Acta Crystallographica, B28, 1899–1903.

Mrose, M.E., and Appleman, D.E. (1962) The crystal structures and crystal chemistry of väyrynenite, $(Mn,Fe)Be(PO_4)(OH)$, and euclase, $AlBe(SiO_4)(OH)$. Zeitschrift für Kristallographie, 117, 16–36.

Newnham, R.E., and Yoon, H.S. (1973) Elastic anisotropy in minerals. Mineralogical Magazine, 39, 78–84.

Ohashi, Yoshikazu. (1982) A program to calculate the strain tensor from two sets of unit-cell parameters. In R.M. Hazen and L.W. Finger, Eds. Comparative crystal chemistry, 92–102. Wiley, New York.

Robinson, K., Gibbs, G.V., and Ribbe, P.H. (1971) Quadratic elongation: A quantitative measure of distortion in coordination polyhedra. Science, 172, 567–570.

Swanson, D.K., Weidner, D.J., Prewitt, C.T., and Kandelin, J.J. (1985) Single crystal compression of γ-Mg_2SiO_4. (abs.) EOS (American Geophysical Union Transactions), 66, 370.

Vaughan, M.T., and Weidner, D.J. (1978) The relationship of elasticity and crystal structure in andalusite and sillimanite. Physics and Chemistry of Minerals, 3, 133–144.

Weidner, D.J., and Vaughan, M.T. (1982) Elasticity of pyroxenes: Effects of composition versus crystal structure. Journal of Geophysical Research, 87, 9349–9354.

Yeganeh-Haeri, A., and Weidner, D.J. (1986) Single crystal elastic moduli of a beryllium silicate: Phenakite Be_2SiO_4. Physics and Chemistry of Minerals, in press.

Yoon, H.S., and Newnham, R.E. (1973) The elastic properties of beryl. Acta Crystallographica, A29, 507–509.

Zachariasen, W.H. (1967) A general theory of X-ray diffraction in crystals. Acta Crystallographica, 23, 558–564.

Zoltai, Tibor. (1960) Classification of silicates and other minerals with tetrahedral structures. American Mineralogist, 45, 960–973.

Manuscript received August 7, 1985
Manuscript accepted March 18, 1986